Supporting Information: Spatially refined aerosol direct radiative forcing efficiencies

Daven K. Henze,* Drew T. Shindell, Farhan Akhtar, Robert J. D. Spurr,
Robert W. Pinder, Dan Loughlin,
Monika Kopacz, Kumaresh Singh, Changsub Shim
*To whom correspondence should be addressed; E-mail: daven.henze@colorado.edu

Contents

First, the accuracy of the adjoint sensitivities from the GEOS-Chem chemical transport model (*47*) are verified through extensive comparisons to finite difference (FD, i.e., conventional forward modeling) sensitivities. We consider ensembles of column models (i.e., no horizontal transport) in order to maximize points of comparison between these two approaches, as well as spot tests of the full 3-D model (testing the full adjoint model for each parameter is not feasible, as it would require $> 10^5$ forward model calculations to generate FD results with which to compare). The agreement of adjoint and FD sensitivities >90% shown in Figs. S1 (a) and (b) demonstrates the adjoint is properly implemented.

We next consider the extent to which linear extrapolations of adjoint sensitivities to estimate DRF (i.e., equation 3) are valid over a range of spatially aggregated perturbations to emissions of specific species. We calculate the aerosol DRF from global anthropogenic sources of SO_2, BC, OC, NH_3, and nitrogen oxides (NO_x) individually, considering increases from pre-industrial conditions and decreases from present day conditions, using 100% perturbations of the present day emissions levels in both cases. Regression of the forward model values against the adjoint estimates (see supplemental Fig. S2) gives an r^2 of 0.76 and a slope of 0.9. The largest relative source of unexplained variance stems from the NO_x perturbations. The adjoint sensitivities significantly under (over) estimate the DRF when considering NO_x increases (decreases) on top of pre-industrial (present-day) values. Therefore, we should consider NO_x sensitivities to be valid over a smaller range of perturbations or we should estimate NO_x DRF from average adjoint values computed at multiple states around the base and perturbed emissions levels. Thus we restrict our attention to emissions of SO_2, BC, OC and NH_3, for which the r^2 is 0.98 and slope 1.1. We also note that forcing estimates for NH_3 calculated around reductions to present day emissions levels vs increases from pre-industrial levels are much larger in the former case owing to broader availability of sulfate and nitrate with which to form aerosol.

Lastly, we consider how well the linearity assumption holds when considering emissions perturbations in individual grid-cells, with magnitudes comparable to expected changes over the next several decades. Results for BC are shown in Fig. S1(c) and for SO_2 in Fig. S1(d); changes in radiative forcing estimated from the adjoint sensitivities correspond well ($r^2 > 0.97$) with changes in radiative forcing calculated explicitly using the full forward model.

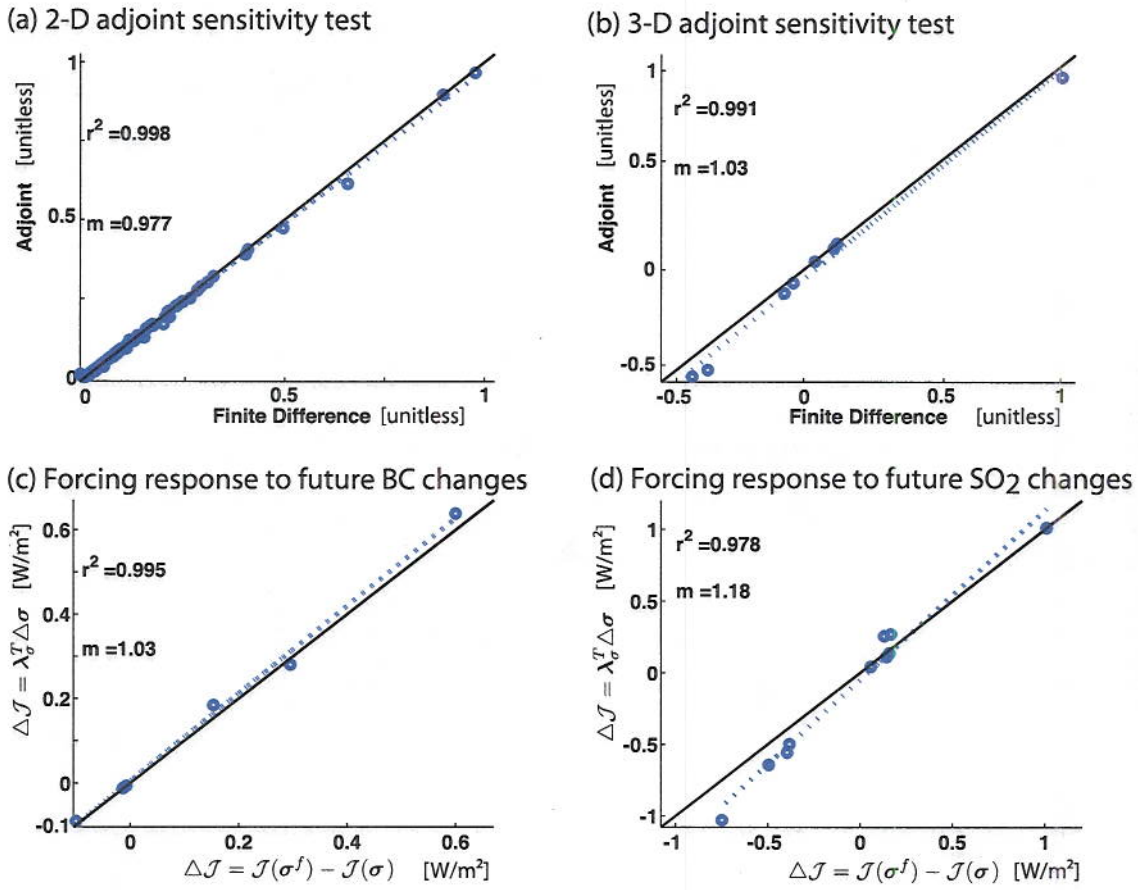

Figure S1: Validation of adjoint model sensitivities (top row) and their applicability (bottom row) for estimating radiative forcing ($\triangle\mathcal{J}$). Solid lines are 1:1, dashed are regressions with given r^2 and slope m. The top row compares normalized adjoint vs finite difference sensitivities for (a) tests of 2-D adjoint column models throughout the globe for the sensitivity of nitrate aerosol to NH_3 emissions and (b) spot tests of the full 3D adjoint model showing the adjoint sensitivity with respect to individual SO_2 emissions in ten locations around the globe compared to finite difference sensitivities. The second row shows the direct aerosol radiative forcing estimated from adjoint sensitivities vs evaluated in the forward model for perturbations following future scenarios for (c) black carbon and (d) SO_2 emissions in different locations around the globe.

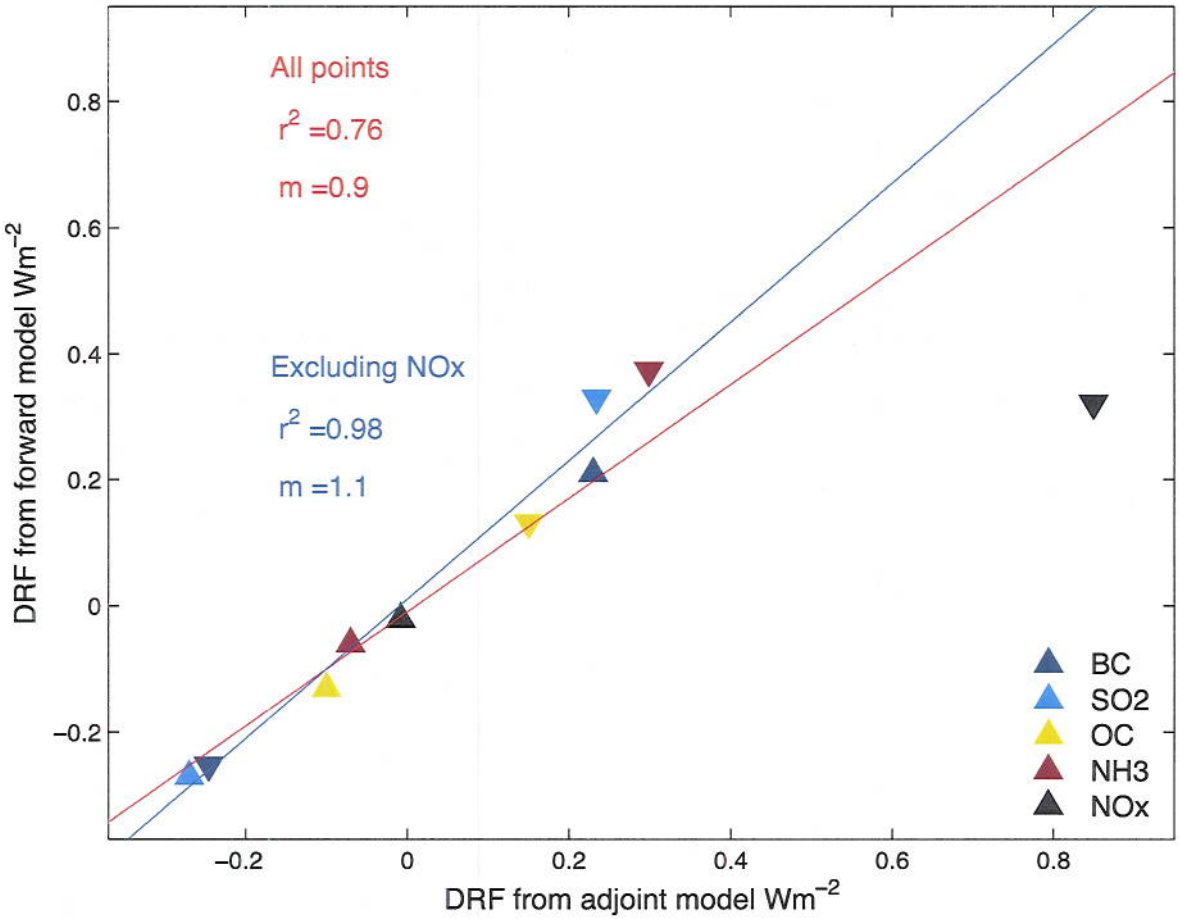

Figure S2: DRF from global perturbations of emissions from specific species, as estimated using the adjoint vs the forward model. Perturbations were 100% the magnitude of present day values, conducted as a positive perturbation to pre-industrial conditions ($\triangle$) and a negative perturbation to present-day conditions ($\triangledown$). Regression lines are shown including all points (red) and including only those unrelated to NO_x (blue).

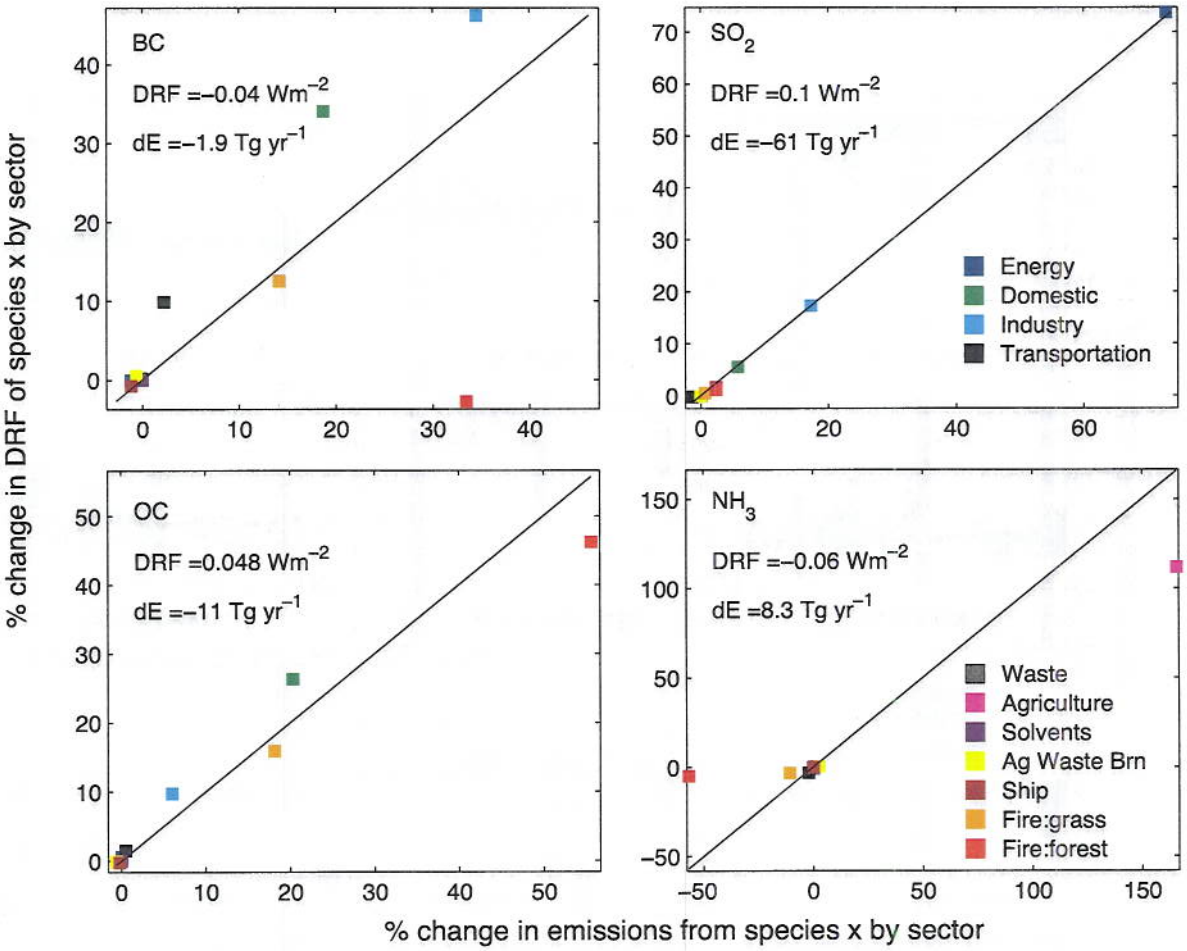

Figure S3: Plotted along the x-axis of each panel are the percent change in emissions for a specific species in each sector summed globally for RCP 4.5 2050 to 2000. On the y-axis is the corresponding percent change in the all-sky aerosol DRF for that sector from each species alone. Each panel also shows the DRF and change in emissions (dE) on which these percentages are based. Note that positive percentages indicate enhancements to the absolute magnitude of net DRF or dE, while negative percentages indicate changes in the direction opposite the net DRF or dE.

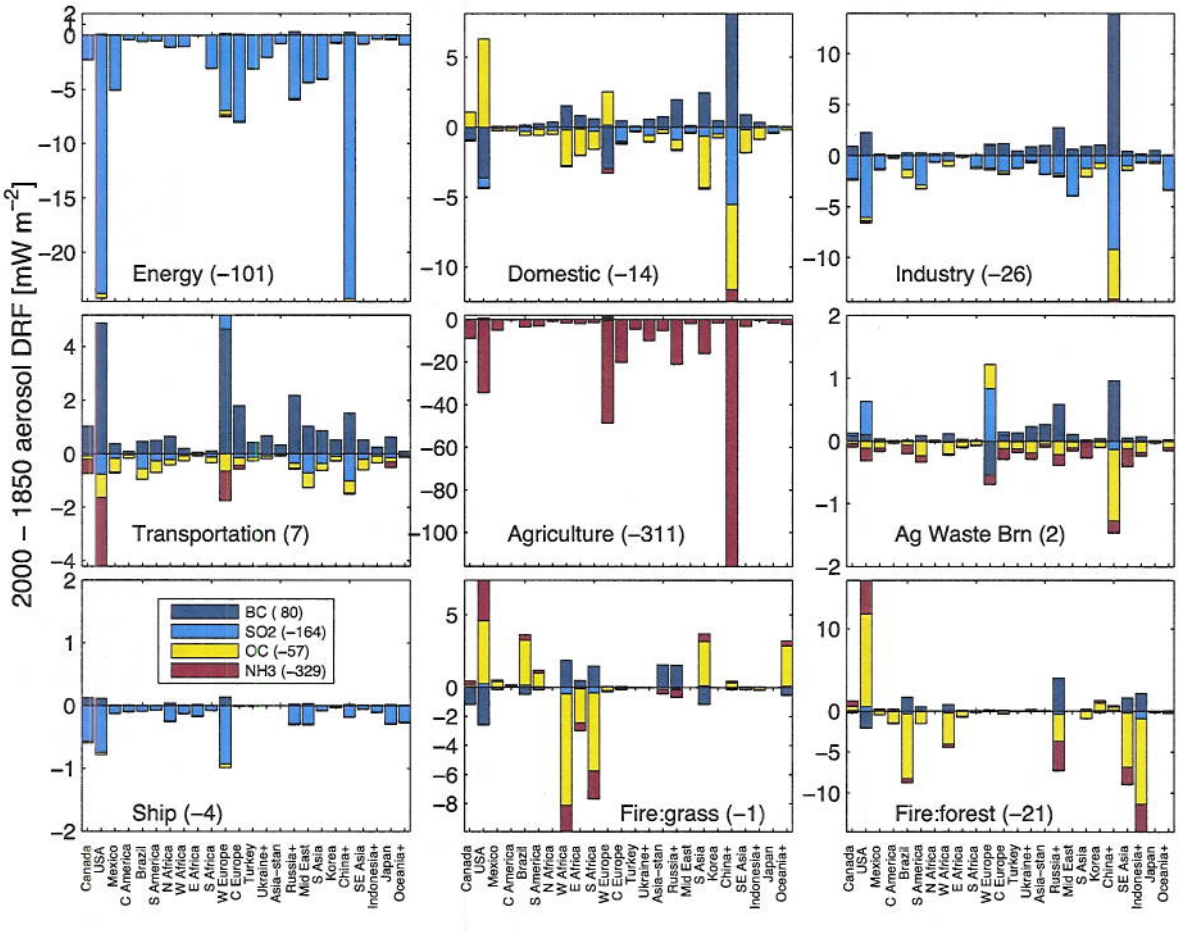

Figure S4: Aerosol DRF of 2000 CMIP5 emissions relative to 1850, for each emission sector and species, lumped by region. Values in parenthesis show the net contribution [mW m^{-2}] from entire sectors or species to the total DRF of -0.47 W m^{-2}.

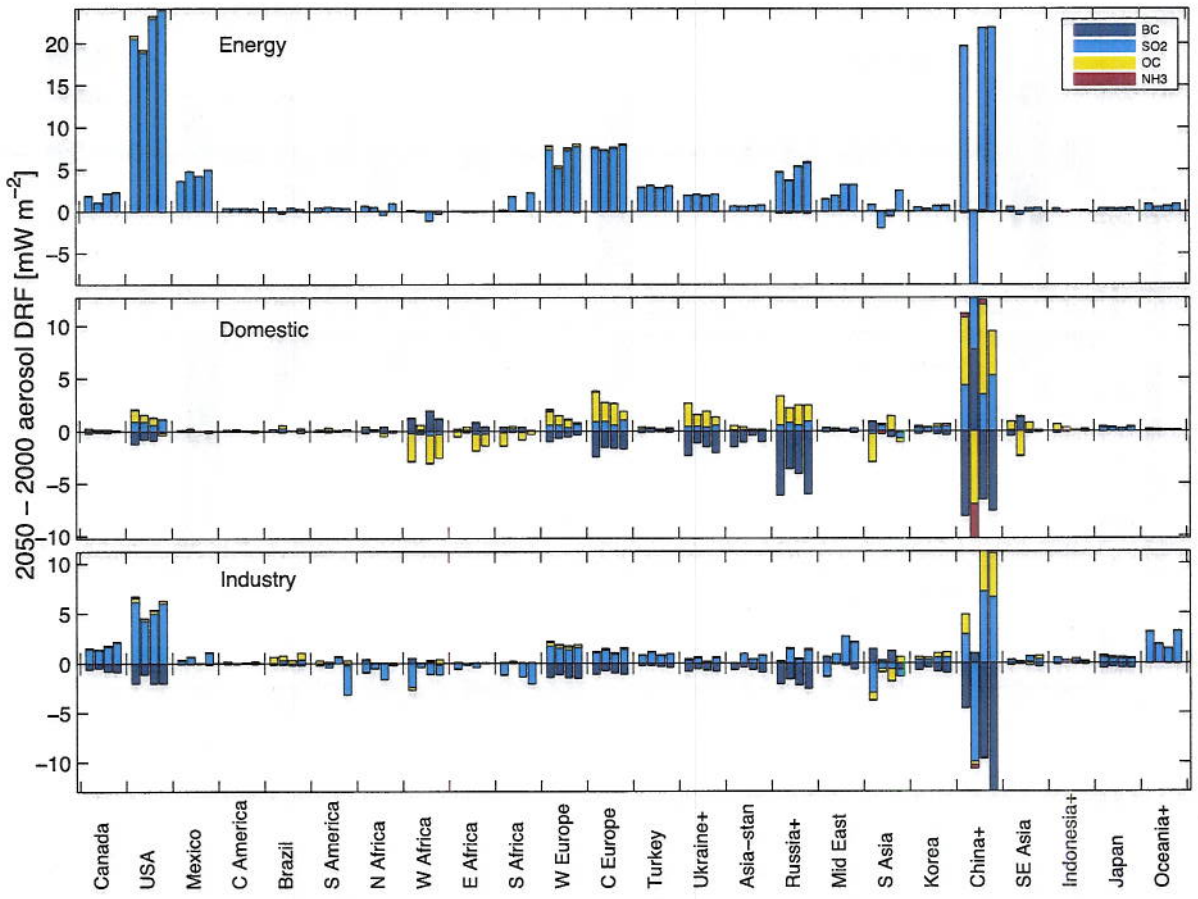

Figure S5: DRF from each region and RCP by sector and species. Within each region, the four bars (from left to right) show the DRFs from RCP 8.5, 6.0, 4.5 and 2.6.

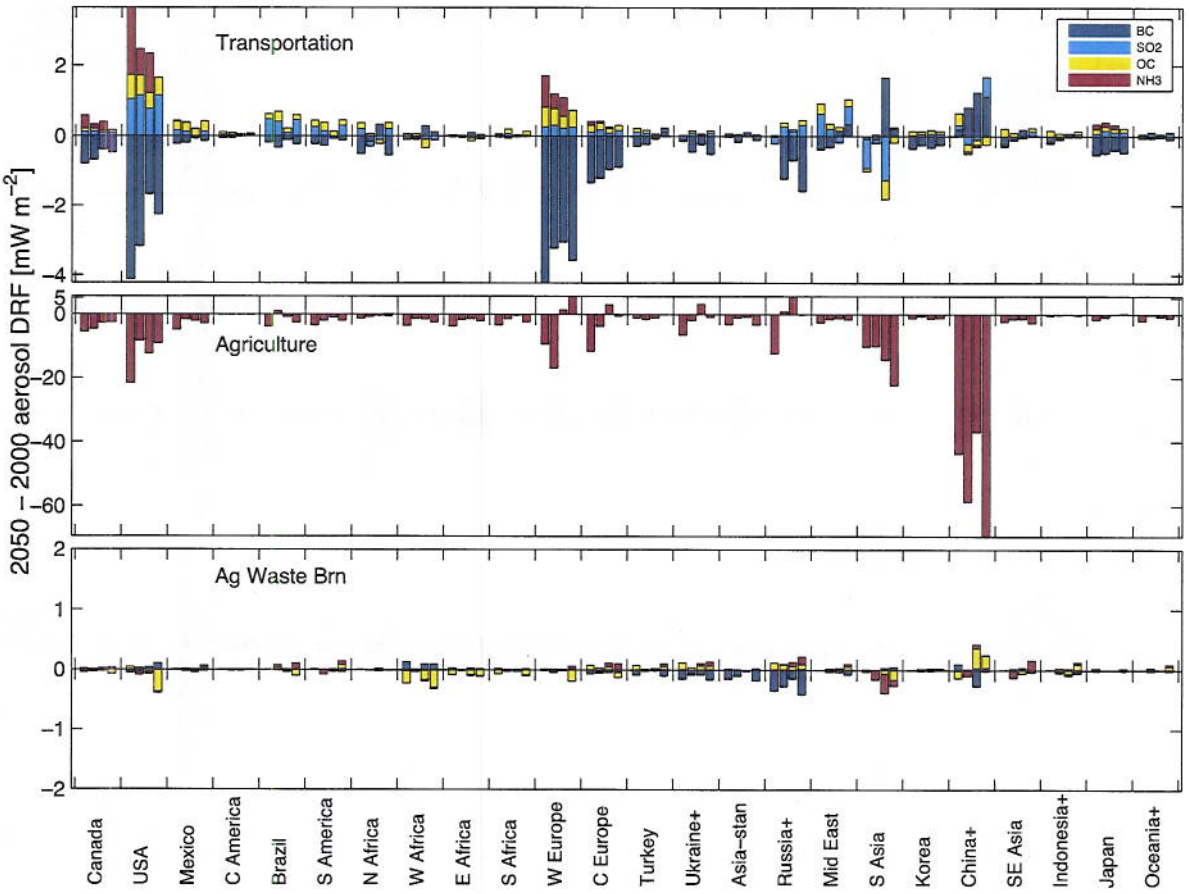

Figure S5: ...continued.

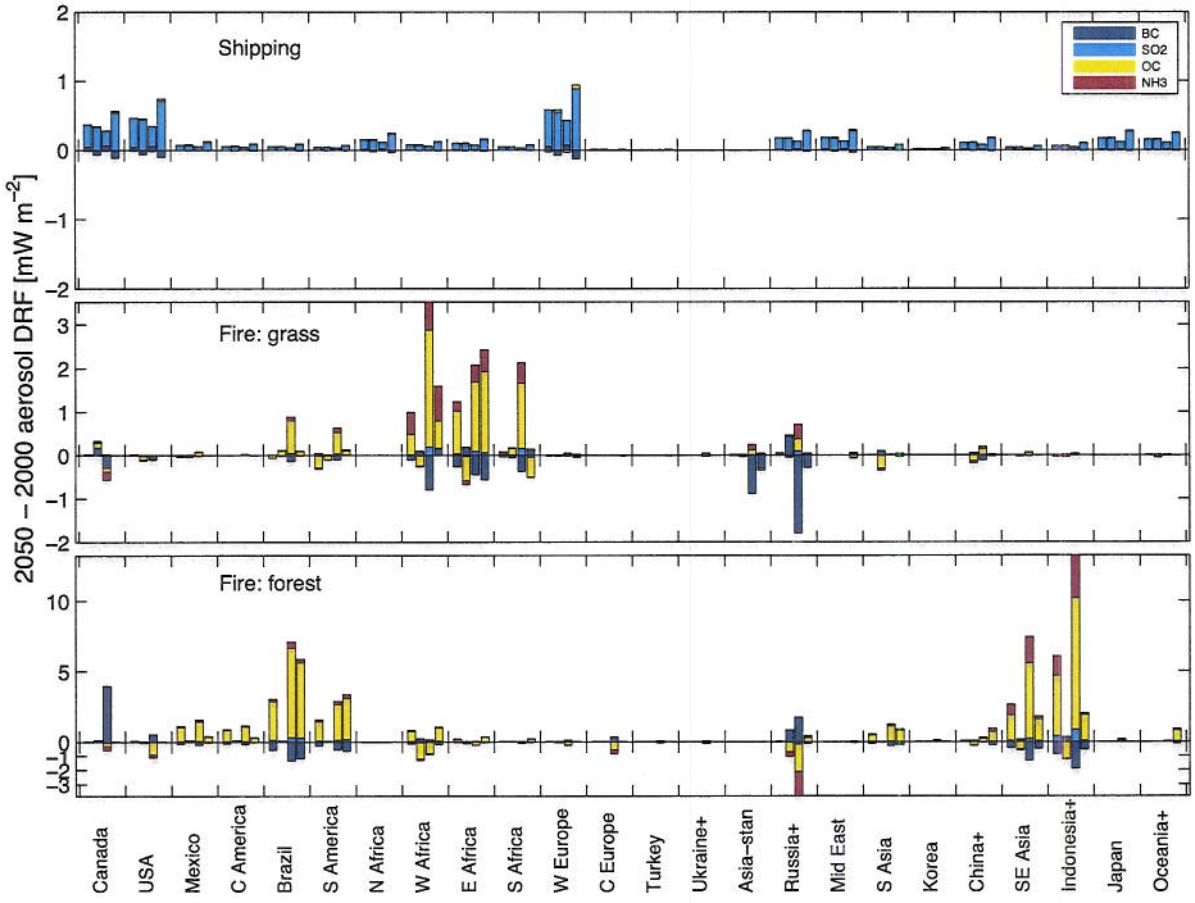

Figure S5: ... continued.